Frontiers in Heat and Mass Transfer (FHMT), 12, 25 (2019)
DOI: 10.5098/hmt.12.25

Global Digital Central
ISSN: 2151-8629

Frontiers in Heat and Mass Transfer

Available at www.ThermalFluidsCentral.org

NUMERICAL SIMULATION FOR INVERSE HEAT CONDUCTION PROBLEM OF SINGLE-LAYER LINING EROSION OF BLAST FURNACE

Fuyong Su[a*], Rui Song[a], Peiwei Ni[a], Zhi Wen[b]

[a] *School of Energy and Environmental Engineering, University of Science and Technology Beijing, Beijing 100083, China*
[b] *Beijing Key Laboratory of Energy Conservation and Emission Reduction for Metallurgical Industry, Beijing, 100083, China*

ABSTRACT

A mathematical model of the inverse heat transfer problem of blast furnace lining is established in this study. Following the identification of the boundary conditions of the model, the inverse problem via the conjugate gradient method was decomposed into three issues: the direct problem, the sensitivity problem, and the adjoint problem. The feasibility of the model was verified through two types of real inner wall boundary shape functions. The effects of the initial inner wall boundary shape function and the number of measuring points are also investigated. Results showed that the accuracy of the inverse solution is independent of the initial inner wall boundary shape function. The number of measuring points exerts some influence on the inversion results. That is, a large number of measuring points equates to a good capture of curves, but an accurate inverse solution also can be obtained with few measuring points, although arranging a large number of points can achieve a slightly better solution. The average relative error of this solution is approximately 3%.

Keywords: *Inverse heat conduction problem, Conjugate gradient method, Lining erosion, Boundary shape*

1. INTRODUCTION

Blast furnaces are important equipment in the steel production process. The erosion problem of blast furnace lining influences the advancement of blast furnaces (Zheng *et al.*, 2009). The problem of the erosion thickness of blast furnace lining is actually an inverse heat conduction problem (IHCP) that involves the calculation of the surface shape of the inner lining using temperatures measured in the blast furnace lining (Zhang *et al.*, 2008).

The IHCP (Hadamard and Morse, 1953; Beck and Woodbury, 2016; Lin and Yang, 2007) is a heat transfer problem whose outcomes are difficult to measure. Since Stolz (Stolz, 1960) published the first paper on the IHCP in 1960, many scientists have explored numerical solutions to the IHCP, such as Tikhonov's regularization method (Qiao *et al.*, 2017), Beck's serialization method, Blackwell's time-marching algorithm method, Weber's space propulsion algorithm method (Blackwell, 1981), Elden's Fourier regularization method (Weber, 1981), and the conjugate gradient method (Isaac, 2018; Amini *et al.*, 2018; Dehghani and Mahdavi-Amiri, 2018). Through these methods, the IHCP has undergone significant advancement in practical engineering and scientific experiment and measurement. The conjugate gradient method (Colaço and Orlande, 2004; Huang and Liu, 2010; Dulikravich and Martin, 2012; Rajaraman *et al.*, 2018) is similar to the steepest descent method and Newton's method as it takes only a first derivative information; however, it overcomes the slow convergence in the steepest descent method and avoids calculating the Hesse matrix in the Newton method. The conjugate gradient method is thus widely used to solve the IHCP.

In this paper, the erosion contour lines of a single-layer blast furnace are calculated on the basis of the temperatures of the internal lining. This problem is a boundary shape IHCP. The mathematical model for solving the inverse heat conduction problem of boundary shape is given in detail, the model is solved by the conjugate gradient method. The influence of different initial inner wall boundary shape function and the number of temperature points on the calculation results is discussed. The work done in this paper lays the foundation for predicting the shape of the inner wall of the blast furnace by measuring the surface temperature of the blast furnace (the wall of the furnace will change due to erosion), and it is will be helpful for the safe production of the blast furnace.

2. MATHEMATICAL MODEL

The calculation area of the mathematical model in this study is shown in Fig. 1. The temperature of the left wall surface was constant, along with the heat flow from the right side surface of the calculation area. The upper and lower walls were under adiabatic conditions. The wall was equipped with several thermocouples for measuring temperature. The measured temperatures are used in the mathematical model to calculate the erosion curve of the inner wall surface (inner wall boundary shape).

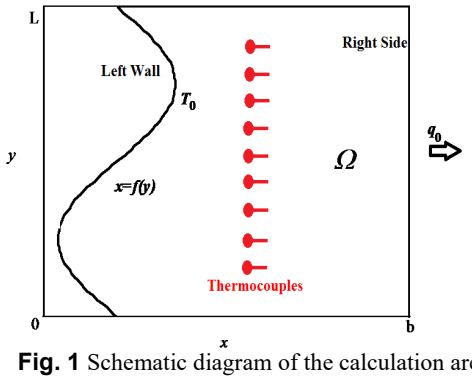

Fig. 1 Schematic diagram of the calculation area

* *Corresponding author. Email: sfyong@ustb.edu.cn*

The conjugate gradient method was used to solve the boundary shape IHCP. The calculation process was divided into the direct problem, the sensitivity problem, and the adjoint problem.

2.1 Direct Problem Model

Under the direct problem model, the temperature distribution throughout the area was calculated by solving the two-dimensional state heat conduction problem with the erosion curve of the inner wall (inner wall boundary shape) being known. The equations and boundary conditions are as follows:

$$\frac{\partial}{\partial x}\left(k\frac{\partial T}{\partial x}\right)+\frac{\partial}{\partial y}\left(k\frac{\partial T}{\partial y}\right)=0 \qquad \subset \Omega \tag{1}$$

$$-k\frac{\partial T}{\partial x}=q_0 \qquad x = b$$

$$T=T_0 \qquad x = f(y)$$

$$\frac{\partial T}{\partial y}=0 \qquad \text{when } y=0 \text{ or } y=L$$

$$T(x_i,y_i)=T_i^c \qquad i=1,2,\cdots m$$

where k is the thermal conductivity, $W\cdot m^{-1}\cdot K^{-1}$; q_0 is the heat flux intensity of the right side, $W\cdot m^{-2}$; T_0 is the temperature of the erosion curve surface of the inner wall, K; T_i^c is the temperature measured by the thermocouple i, K; and m is the number of the thermocouple.

2.2 Inverse Problem Model

Under the inverse problem model, the inner wall boundary shape was calculated using the measuring point temperatures. We calculated the temperatures by solving the direct problem with the assumption that the inner wall boundary shape was $x=f(y)$. We also calculated the square of the differences between the measured temperatures and the calculated temperatures. When the square was minimum, the supposed inner wall boundary shape was the real inner wall boundary shape. The equation of the inverse problem model is as follows:

$$J(f(y))=\left\|T_i-T_i^c\right\|^2=\sum_{i=1}^{m}\left[T_i(x_i,y_i)-T_i^c(x_i,y_i)\right]^2 \tag{2}$$

where $T_i(x_i,y_i)$ denotes the calculated temperatures at point i, K; and $T_i^c(x_i,y_i)$ denotes the measured temperatures at point i, K.

2.3 Sensitivity Problem Model

Under the sensitivity problem model, the incremental temperature ($\Delta T(x,y)$) when the inner wall boundary shape changed ($f(y)+\Delta f(y)$) was calculated. The equations and boundary conditions of the sensitivity problem model are as follows:

$$\frac{\partial}{\partial x}\left(k\frac{\partial \Delta T}{\partial x}\right)+\frac{\partial}{\partial y}\left(k\frac{\partial \Delta T}{\partial y}\right)=0 \qquad \subset \Omega \tag{3}$$

$$-k\frac{\partial \Delta T}{\partial x}=0 \qquad x = b$$

$$\Delta T=\Delta f\frac{\partial T}{\partial x} \qquad x = f(y)$$

$$\frac{\partial \Delta T}{\partial y}=0 \qquad y=0$$

$$\frac{\partial \Delta T}{\partial y}=0 \qquad y=L$$

2.4 Adjoint Problem Model

The adjoint problem is a functional derivative problem that aims to obtain the gradient of the objective function. First, we used Equation 1 (the direct problem model) multiplied by a Lagrangian $\lambda(x,y)$ (the adjoint function). Second, we performed regional integration and added it to Equation 2 (the inverse problem model). Third, we used $T+\Delta T$ to replace T and $f(y)+\Delta f(y)$ to replace $f(y)$. Then, we obtained the function $\Delta J[f(y)]$. Finally, we obtained the equations of the adjoint problem model when $\Delta J[f(y)]$ approached 0 by using the boundary conditions of the sensitivity problem model.

$$\frac{\partial^2\lambda}{\partial x^2}+\frac{\partial^2\lambda}{\partial y^2}=0 \qquad \subset \Omega \tag{4}$$

$$-\frac{\partial\lambda}{\partial y}=2\left(T_i-T_i^c\right)\delta(y-y_i) \qquad x = b$$

$$\lambda=0 \qquad x = f(y)$$

$$\frac{\partial\lambda}{\partial y}=0 \qquad y=0$$

$$\frac{\partial\lambda}{\partial y}=0 \qquad y=L$$

After determining the values of $\lambda(x,y)$ (the adjoint function), we obtained the following derivative of the objective function:

$$J'(f(y))=-\frac{\partial\lambda}{\partial x}\cdot\frac{\partial T}{\partial x}\bigg|_{x=f(y)} \tag{5}$$

2.5 Iterative Search Method

The conjugate gradient method can be employed to construct a set of conjugate directions by using the gradient at known points and searching along the conjugate directions. The result is the minimum value of the objective function. The equations of the iterative search model are as follows:

$$d_1=-J_1' \qquad n=1 \tag{6}$$

$$d_n=-J_n'+\beta_n d_{n-1} \qquad n\geq 2 \tag{7}$$

where d_n is the n-th search direction, which is the negative gradient direction in the first search; J_n' is the gradient direction; and β_n is the conjugated factor, which could be calculated with the following equation:

$$\beta_n=\frac{\int_{y=0}^{L}\left(J_n'\right)^2dy}{\int_{y=0}^{L}\left(J_{n-1}'\right)^2dy} \qquad (n\geq 2) \tag{8}$$

The change of the inner wall boundary shape can be obtained from the search step α_n and the search direction d_n. Inner wall boundary shape $f(y)$ could be calculated with the following equation:

$$f_{n+1}=f_n+\alpha_n d_n \tag{9}$$

where α_n is the search step, which could be calculated with the following equation:

$$\alpha_n=\frac{\sum_{i=1}^{m}\left(T_i-T_i^c\right)\Delta T_i}{\sum_{i=1}^{m}\left(T_i-T_i^c\right)^2} \tag{10}$$

The steps of the conjugate gradient method are as follows:

Step 1: The initial inner wall boundary shape $f(y)$ is considered, and the temperatures $T_i(x_i,y_i)$ of the measuring points are calculated by solving Equation 1 (the direct problem model).

Step 2: The measured temperatures ($T_i^c(x_i,y_i)$) and calculated temperatures ($T_i(x_i,y_i)$) are compared. If the temperatures meet the convergence conditions ($J(f(y))<\varepsilon$) of Equation 2 (the inverse problem model), then $f(y)$ is the real inner wall boundary shape; otherwise, the next step is performed.

Global Digital Central
ISSN: 2151-8629

Step 3: The adjoint problem model is solved, the values of the adjoint function in all areas are obtained, and the gradient ($J'(f(y))$) of the objective function is determined.

Step 4: The conjugated factor and search direction are calculated.

Step 5: Let $\Delta f=d_n$. The incremental temperature ΔT is calculated by solving the sensitivity problem model (Equation 3).

Step 6: The search step is calculated by solving Equation 10. The new inner wall boundary shape is determined by solving Equation 9, and the new temperatures ($T_i(x_i,y_i)$) are determined by solving Equation 1. Then return to step 2, determine whether the temperatures meet the convergence conditions of Equation 2 again.

3. MODEL VALIDATION AND ANALYSIS OF SIMULATION RESULTS

3.1 Model Validation Criteria

In this study, the erosion of the blast furnace lining served as the background. Thus, the initial parameters were set as follows:

The inner wall surface temperature T_0 was 1150 °C (T_0=1150 °C). No erosion was noted in the initial phase. Thus, thickness b in the x-axis direction was 0.5 m (b=0.5 m), and length L in the y-axis direction was 1 m (L=1 m). The measuring points were evenly arranged, and the total number M was 11 (M=11). The size of the study area was 0.5 m × 1 m. The number of mesh was 50 × 100, and the mesh size was 1 cm × 1 cm. We supposed that in the beginning, the inner wall boundary shape function was x=f(y)=0. The heat flux intensity q_0 was 50000 W·m^{-2} (q_0=50000 W·m^{-2}).

3.2 Analysis of Results

(1) The real inner wall boundary shape function 1

$$x = f(y) = 0.35 - 0.1\sin(2\pi y) \qquad 0 \le y \le 1 \tag{11}$$

Under this real shape function, the temperatures of the study area are shown in Fig. 2.

On the basis of the temperatures of 11 measuring points, we solved the boundary shape of the inner wall by using the conjugate gradient method. When the temperatures met the convergence conditions, we obtained the calculated inner wall boundary shape. By comparing the real shape and the calculated shape, we concluded that the relative error for each corresponding point was approximately 1% and that the average relative error was 0.83%. The real shape and the calculated shape are shown in Fig. 3.

(2) The real inner wall boundary shape function 2

$$x = f(y) = \begin{cases} 0.45 - 0.4y & 0 \le y < 0.5 \\ 0.25 + 0.4(y - 0.5) & 0.5 \le y \le 1 \end{cases} \tag{12}$$

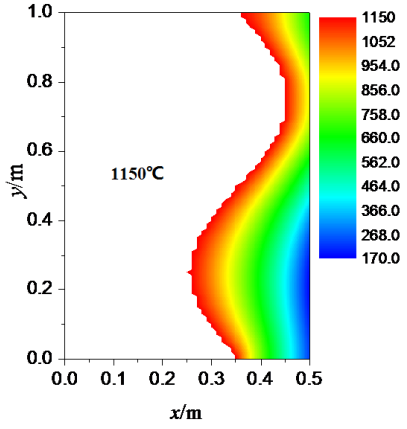

Fig. 2 Temperatures of the study area

Under this real inner wall boundary shape function, the temperatures of the study area are shown in Fig. 4.

On the basis of the temperatures of 11 measuring points, we solved the boundary shape of the inner wall by using the conjugate gradient method. When the temperatures met the convergence conditions, we obtained the calculated inner wall boundary shape. By comparing the real shape and the calculated shape, we noted that the relative error for each corresponding point was about 0.1%–2% and the average relative error was 0.73%. The real shape and calculated shape are shown in Fig. 5.

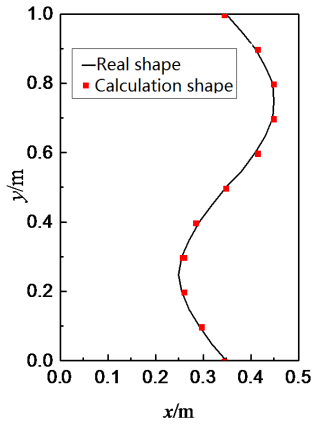

Fig. 3 Real shape and calculated shape

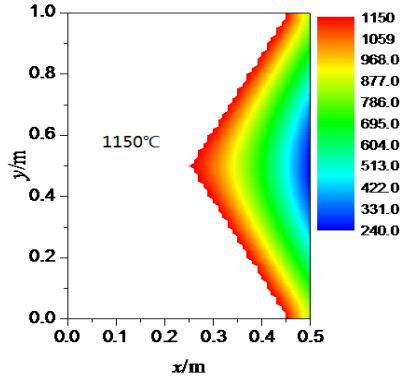

Fig. 4 Temperatures of the study area

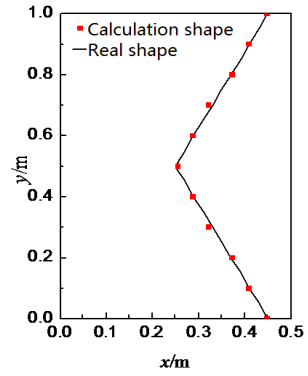

Fig. 5 Real shape and calculated shape

In the two types of real inner wall boundary shape function, all relative errors were less than 3%. Thus, we believed that the mathematical model we established in this work was accurate.

Global Digital Central
ISSN: 2151-8629

3.3 Effect of the Number of Measuring Points

We kept the other parameters unchanged, increased the number of measuring points (M) from 11 to 21, and recalculated the inner wall boundary shape. The results are as follows.

Under the real inner wall boundary shape function 1, the average relative error when M was increased from 11 to 21 changed from 0.83% to 0.81%. The real shape and calculated shape are shown in Fig. 6.

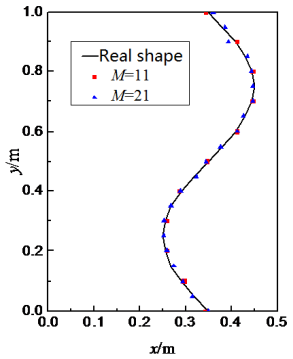

Fig. 6 Real shape and calculated shape (M=11 and M=21)

Under the real inner wall boundary shape function 2, the average relative error when M was increased from 11 to 21 changed from 0.73% to 0.66%. The real shape and calculated shape are shown in Fig. 7.

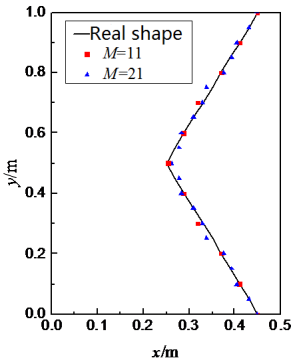

Fig. 7 Real shape and calculated shape (M=11 and M=21)

The results showed that the calculated shapes improved when the number of measuring points (M) changed from 11 to 21. That is, the average relative errors changed from 0.83% to 0.81% and from 0.73% to 0.66% under the real inner wall boundary shape functions 1 and 2, respectively. Furthermore, all relative errors were less than 3%. Thus, increasing the number of measuring points could slightly increase calculation accuracy.

3.4 Effect of Initial Inner Wall Boundary Shape Function

We supposed that the initial inner wall boundary shape function was x=f(y)=0 in the beginning. At this stage, we kept the other parameters unchanged and changed the initial inner wall boundary shape function. The new initial inner wall boundary shape function is as follows:

$$x = f(y) = b - k\frac{T_0 - T_i^c}{q_0} \tag{13}$$

where q_0 is the heat flux intensity of the right side, $W \cdot m^{-2}$; k is the thermal conductivity, $W \cdot m^{-1} \cdot K^{-1}$; T_0 is the temperature of the erosion curve surface of the inner wall, K; T_i^c is the temperature measured by the thermocouple i, K; and b is the thickness of the x-direction.

Under the real inner wall boundary shape function 1, the average relative error changed from 0.83% to 0.66% when we changed the initial inner wall boundary shape function. The real shape and calculated shape are shown in Fig. 8. "Calculated shape 1" was calculated on the basis of the original initial inner wall boundary shape function (x=f(y)=0), and "calculated shape 2" was calculated on the basis of the new initial inner wall boundary shape function.

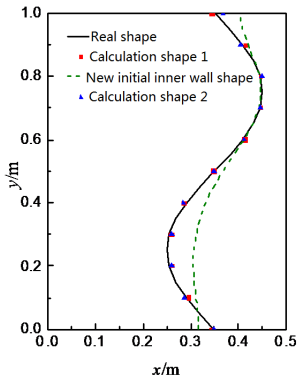

Fig. 8 Real shape and calculated shape (two initial inner wall shape functions)

Under the real inner wall boundary shape function 2, the average relative error changed from 0.73% to 0.74% when we changed the initial inner wall boundary shape function. The real shape and calculated shape are shown in Fig. 9. "Calculated shape 1" was calculated on the basis of the original initial inner wall boundary shape function (x=f(y)=0), and "calculated shape 2" was calculated on the basis of the new initial inner wall boundary shape function.

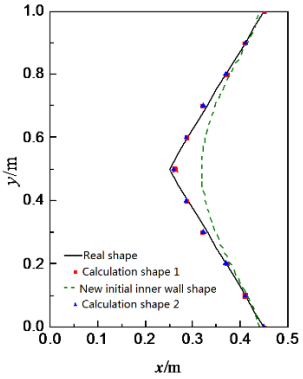

Fig. 9 Real shape and calculated shape (two initial inner wall shape functions)

The results showed that the calculated shapes remained nearly the same when we changed the initial inner wall boundary shape function. That is, the average relative errors changed from 0.83% to 0.66% and from 0.73% to 0.74% on the basis of the real inner wall boundary shape functions 1 and 2, respectively. Furthermore, all relative errors were less than 3% under the two initial inner wall shape boundary functions based on the two types of real shape function. Thus, the initial inner wall boundary shape function had little effect on calculation accuracy.

4. CONCLUSION

A mathematical model of the IHCP of blast furnace lining was established in this work. After determining the boundary conditions of the model, the inverse problem via the conjugate gradient method was decomposed into three issues: the direct problem, the sensitivity problem, and the adjoint problem. By solving the mathematical model, we arrived at the following conclusions:

(1) Under the two types of real inner wall boundary shape function, the calculated shapes were basically the same as the real shapes. All relative errors were less than 3%. Thus, we believed that the mathematical model established in this work was accurate.

(2) The calculated inner wall boundary shapes improved when the number of measuring points (M) was changed from 11 to 21. That is, the average relative errors changed from 0.83% to 0.81% and from 0.73% to 0.66% on the basis of the real inner wall boundary shape functions 1 and 2, respectively. Furthermore, all relative errors were less than 3%. Thus, increasing the number of measuring points could slightly increase calculation accuracy.

(3) The influence of the initial inner wall boundary shape function is studied. When the inner wall boundary shape function is changed, the relative error changes under the two kinds of function are irregular (0. 83% is reduced to 0.66% and 0.73% is increased to 0. 74%, compared to the original inner wall boundary shape function), and all relative errors are less than 3%, so this paper considers that the initial guess curve has little effect on the calculation accuracy of the model established in this paper.

ACKNOWLEDGMENTS

This research is financially supported by The National Key R&D Program of China (No. 2016YFC0401200). National Key R&D Program of China (2018YFB0605900).

REFERENCES

Amini, K., Faramarzi, P., and Pirfalah, N., 2018, "A Modified Hestenes–Stiefel Conjugate Gradient Method with an Optimal Property", *Optimization Methods & Software,* **1**, 1-13.
http://dx.doi.org/10.1080/10556788.2018.1457150

Blackwell, B. F., 1981, "Efficient Technique for the Numerical Solution of the One-Dimensional Inverse Problem of Heat Conduction", *Numerical heat transfer*, **4**, 229-238.
http://dx.doi.org/10.1080/01495728108961789

Beck, J. V., and Woodbury, K. A., 2016, "Inverse Heat Conduction Problem: Sensitivity Coefficient Insights, Filter Coefficients, and Intrinsic Verification", *International Journal of Heat and Mass Transfer*, **97**, 578-588.
http://dx.doi.org/10.1016/j.ijheatmasstransfer.2016.02.034

Colaço, M. J., and Orlande, H. R., 2004, "Inverse Natural Convection Problem of Simultaneous Estimation of Two Boundary Heat Fluxes in Irregular Cavities", *International Journal of Heat and Mass Transfer*, **47**, 1201-1215.
http://dx.doi.org/10.1016/j.ijheatmasstransfer.2003.09.007

Dulikravich, G. S., and Martin, T. J., 2012, "Inverse Design of Super-Elliptic Cooling Passages in Coated Turbine Blade Airfoils", *Journal of Thermophysics & Heat Transfer,* **8**, 288-294.
http://dx.doi.org/10.2514/3.536

Dehghani, R., and Mahdavi-Amiri, N., 2018, "Scaled Nonlinear Conjugate Gradient Methods for Nonlinear Least Squares Problems", *Numerical Algorithms*, **79**, 1-20.
http://dx.doi.org/10.1007/s11075-018-0591-2

Hadamard, J., and Morse, P. M., 1953, "Lectures on Cauchy's Problem in Linear Partial Differential Equations", *Physics Today,* **6**, 18-18.
http://dx.doi.org/10.1063/1.3061337

Huang, C. H., and Liu, C. Y., 2010, "A Three-Dimensional Inverse Geometry Problem in Estimating Simultaneously Two Interfacial Configurations in a Composite Domain", *International Journal of Heat and Mass Transfer,* **53**, 48-57.
http://dx.doi.org/10.1016/j.ijheatmasstransfer.2009.10.009

Isaac, C. W., 2018, "Proper Generalized Decomposition Method for Solving Fisher-Type Equation and Heat Equation", *Mathematical Models & Computer Simulations,* **10**, 120-133.
http://dx.doi.org/10.1134/S2070048218010039

Lin, D. T., and Yang, C. Y., 2007, "The Estimation of the Strength of the Heat Source in the Heat Conduction Problems", *Applied Mathematical Modelling*, **31**, 2696-2710.
http://dx.doi.org/10.1016/j.apm.2006.10.022

Qiao, B., Zhang, X., Gao, J., Liu, R., and Chen, X., 2017, "Sparse Deconvolution for the Large-Scale Ill-Posed Inverse Problem of Impact Force Reconstruction", *Mechanical Systems and Signal Processing*, **83**, 93-115.
http://dx.doi.org/10.1016/j.ymssp.2016.05.046

Rajaraman, R., Gowsalya, L. A., and Velraj, R., 2018, "Interfacial Heat Transfer Coefficient Estimation During Solidification of Rectangular Aluminum Alloy Casting Using Two Different Inverse Methods", *Frontiers in Heat and Mass Transfer,* **11**, 1-8.
http://dx.doi.org/10.5098/hmt.11.23

Stolz G., 1960, "Numerical Solutions to an Inverse Problem of Heat Conduction for Simple Shapes", *Journal of Heat Transfer,* **82**, 20-25.
http://dx.doi.org/10.1115/1.3679871

Weber, C. F., 1981, "Analysis and Solution of the Ill-Posed Inverse Heat Conduction Problem", *International Journal of Heat and Mass Transfer,* **24**, 1783-1792.
http://dx.doi.org/10.1016/0017-9310(81)90144-7

Zhang, Y., Deshpande, R., Huang, D., Chaubal, P., and Zhou, C. Q., 2008, "Numerical Analysis of Blast Furnace Hearth Inner Profile by Using CFD and Heat Transfer Model for Different Time Periods", *International Journal of Heat and Mass Transfer,* **51**, 186-197.
http://dx.doi.org/10.1016/j.ijheatmasstransfer.2007.04.052

Zheng, K., Wen, Z., Liu, X., Ren, Y., Wu, W., and Qiu, H., 2009, "Research Status and Development Trend of Numerical Simulation on Blast Furnace Lining Erosion", *ISIJ international*, **49**, 1277-1282.
http://dx.doi.org/10.2355/isijinternational.49.1277